

CO₂ Corrosion Inhibition by Imidazoline Derivatives Based on Coconut Oil

L.M. Rivera-Grau¹, M. Casales², I. Regla^{2,3}, D. M. Ortega-Toledo², J.G. Gonzalez-Rodriguez^{1,*},
L. Martinez Gomez²

¹ Universidad Autonoma del Estado de Morelos, CIICAp, AV. Universidad 1001,
62209-Cuernavaca, Mor., Mexico

² Universidad Nacional Autonoma de Mexico, Instituto de Ciencias Fisicas, AV. Universidad s/n,
Cuernavaca, Mor., Mexico

³ Universidad Nacional Autonoma de Mexico, Facultad de Estudios Superiores Zaragoza, Mexico
D.F., Mexico

*E-mail: ggonzalez@uaem.mx

Received: 1 October 2012 / Accepted: 22 October 2012 / Published: 1 December 2012

A coconut-oil modified hydroxyethyl-imidazoline has been synthesized and used as an inhibitor of CO₂ corrosion for carbon steel in 3% NaCl solution at 50°C. Testing techniques includes potentiodynamic polarization curves, linear polarization resistance, electrochemical impedance spectroscopy, and electrochemical noise measurements by using 20 ppm of inhibitor. Results indicated that, even when the commercial imidazoline decreased the corrosion rate with efficiency higher than 400%, the coconut-oil modified imidazoline reduced the corrosion rate by more than 85%, giving promising results for using it as a green corrosion inhibitor.

Keywords: Green inhibitor, acidic corrosion, electrochemical noise.

1. INTRODUCTION

Carbon dioxide (CO₂) corrosion of carbon steel pipelines and equipment in the oil and gas industry has been given much attention in recent years because of an increased tendency to inject CO₂ into oil wells to reduce the viscosity of oil and increase the its production [1-2]. The presence of H₂S and CO₂ and impurities such as chlorides, cyanides, etc... promotes the corrosion phenomenon. Recently, the CO₂ corrosion becomes even more serious along with increasing the CO₂ and water in oil field as result of exploration in middle or later period and using the technique of enhanced oil recovery (EOR) [3-5]. During these corrosion processes, the carbon steel surface can be covered by a corrosion

scale (FeCO_3), which could slow down the corrosion rate and could protect the substrate from further corrosion [6, 7].

The injection of corrosion inhibitor is a standard practice in oil and gas production systems to control internal corrosion of carbon steel structures. Nitrogen-based organic inhibitors, such as imidazolines or their salts have been successfully used in these applications even without an understanding of the inhibition mechanism [8-15]. The corrosion inhibition of organic compounds is related to their adsorption properties. Adsorption depends on the nature and the state of the metal surface, on the type of corrosive environment and on the chemical structure of the inhibitor [13]. Different derivatives from imidazolines are employed as steel corrosion inhibitors. Even though they have been specially employed in the oil industry, only recently a respectable amount of studies have been undertaken to understand how they work. [9,14-20]. These inhibitors are evaluated in field conditions or simulated media by weight loss measurements, which do not reflect the changes experienced by the corrosion mechanism whatsoever. Related studies have used electrochemical techniques such as potentiodynamic techniques, electrochemical impedance spectroscopy and open circuit potential measurements, which show significant changes in the corrosion due to the presence of inhibitors [21-24].

Recently Yoo et al. [25] evaluated a bio-diesel-based imidazoline, namely 2-(2-alkyl-4,5-dihydro-1H-imidazol-1-yl)ethanol, as corrosion inhibitor of mild steel in 1.0 M hydrochloric acid (HCl) and compared with the same imidazoline but prepared with petroleum-based chemicals. It was found that when the bio-diesel-based imidazoline had a concentration over 100 ppm, it acted as an effective corrosion inhibitor. An undergoing research project in our laboratory deals with the possibility of using coconut oil as corrosion inhibitors. Thus, the aim of this work is to evaluate the corrosion inhibition performance of a coco-modified imidazoline in an CO_2 -containing environment.

2. EXPERIMENTAL

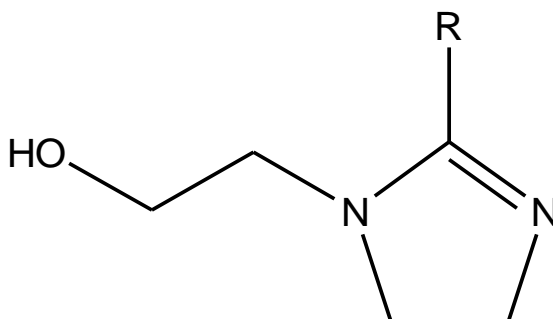


Figure 1. General structure of hydroxyethyl imidazoline, where R is an alkyl chain derivative.

Material tested was a 1018 carbon steel cylinder measuring 25 mm in length and 5.0 mm diameter. Before testing, the electrode was polished to 600 grit SIC emery paper and then cleaned with alcohol, acetone and distilled water. Inhibitors used in this work include a commercial

hydroxyethyl-imidazoline (inhibitor A) and an aminoethyl-amine imidazoline, (inhibitor B) which resulted from modifying inhibitor A with coconut. The general structure of both inhibitors is shown on Fig. 1. A mixture of distilled coconut biodiesel (59-120 ° C / 0.05 mmHg) 2.22 g and 0.936 g of 2-(2-aminoethylamino)ethanol were heated and magnetically stirred at 140 ° C during 9 hours at atmospheric pressure and 3 hours at a reduced pressure (20 mm Hg). The reaction mixture was distilled at the Kugelrohr apparatus under reduced pressure (235 ° C / 0.05 mmHg) to obtain 1.42 g of coconut imidazoline mixture. Inhibitors were dissolved in pure 2-propanol. The concentration of the inhibitors used in this work was 25 ppm and the temperature kept at 50°C. Testing solution consists of 3% NaCl solution, heated, de-aerated by purging with CO₂ gas during 2 hours prior the experiment and kept bubbling throughout the experiment. Inhibitor is added 2 hours after pre-corroding the specimens in the CO₂-containing solution. Electrochemical techniques employed included potentiodynamic polarization curves, linear polarization resistance, LPR, and electrochemical impedance spectroscopy, EIS, and electrochemical noise, EN, measurements. Polarization curves were recorded at a constant sweep rate of 1 mV/s and the scanning range was from -300 to +300 mV respect to the open circuit potential, E_{corr}. Measurements were obtained by using a conventional three electrodes glass cell with two graphite electrodes symmetrically distributed and a saturated calomel electrode (SCE) as reference with a Lugging capillary bridge. Inhibition efficiencies ($E(\%)$) were determined from the corrosion current densities calculated by the Tafel extrapolation method according to the following equation

$$E(\%) = \frac{i_i - i_b}{i_i} \times 100 \quad (1)$$

where i_b is the corrosion rate without inhibitor and i_i the corrosion rate in the solution with inhibitor. LPR measurements were carried out by polarizing the specimen from +10 to -10 mV respect to E_{corr}, at a scanning rate of 1 mV/s. Inhibition efficiencies [$E(\%)$] were determined according to the following equation:

$$E(\%) = \frac{R_{p,i} - R_{p,b}}{R_{p,i}} \times 100 \quad (2)$$

where $R_{p,b}$ is the linear polarization resistance without inhibitor and $R_{p,i}$ is the linear polarization resistance with inhibitor. Electrochemical impedance spectroscopy tests were carried out at E_{corr} by using a signal with an amplitude of 10 mV and a frequency interval of 0.1-100KHz. An ACM potentiostat controlled by a desk top computer was used for the LPR tests and polarization curves, whereas for the EIS measurements, a model PC4 300 Gamry potentiostat was used. Finally, EN measurements for both current and potential were recorded using two identical working electrodes and a saturated calomel reference electrode (SCE). Electrochemical noise measurements were carried out by simultaneously recording potential and current fluctuations at a sampling rate of 1 point per second for a period of 1024 seconds. A fully automated zero resistance ammeter (ZRA) from ACM instruments was used in this case. Removal of the DC trend from the raw noise data was the first step in the noise analysis. To accomplish this, a least square fitting method was used. Finally, the noise

resistance value, R_n , was calculated as the ratio of potential noise standard deviation, σ_v , over current noise standard deviation, σ_i .

3. RESULTS AND DISCUSSION

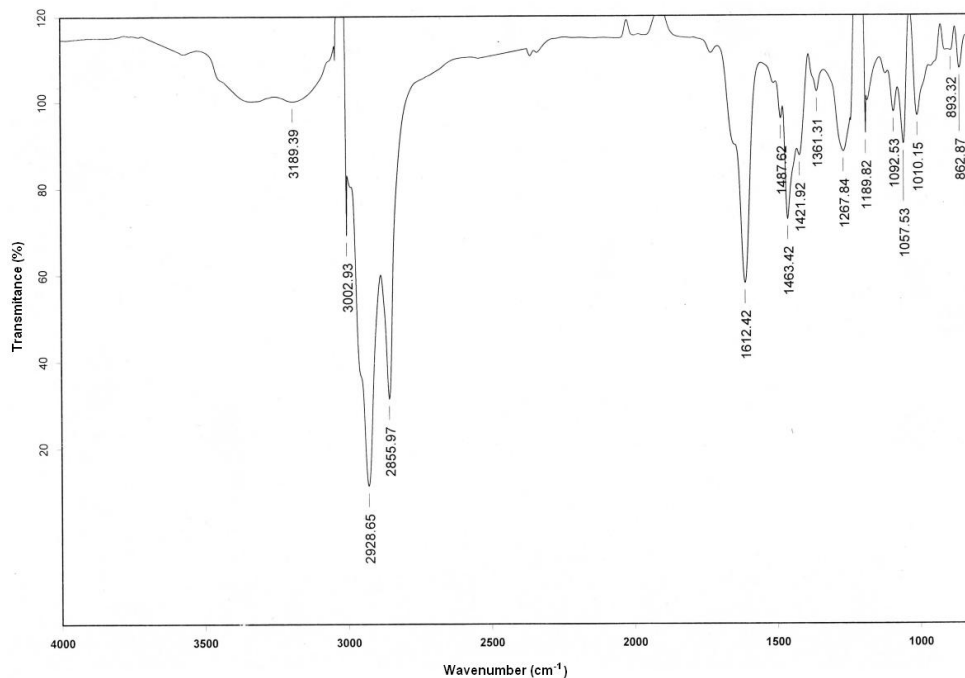


Figure 2. Infrared spectrum of commercial Hidroxitielimidazoline (Inhibitor A).

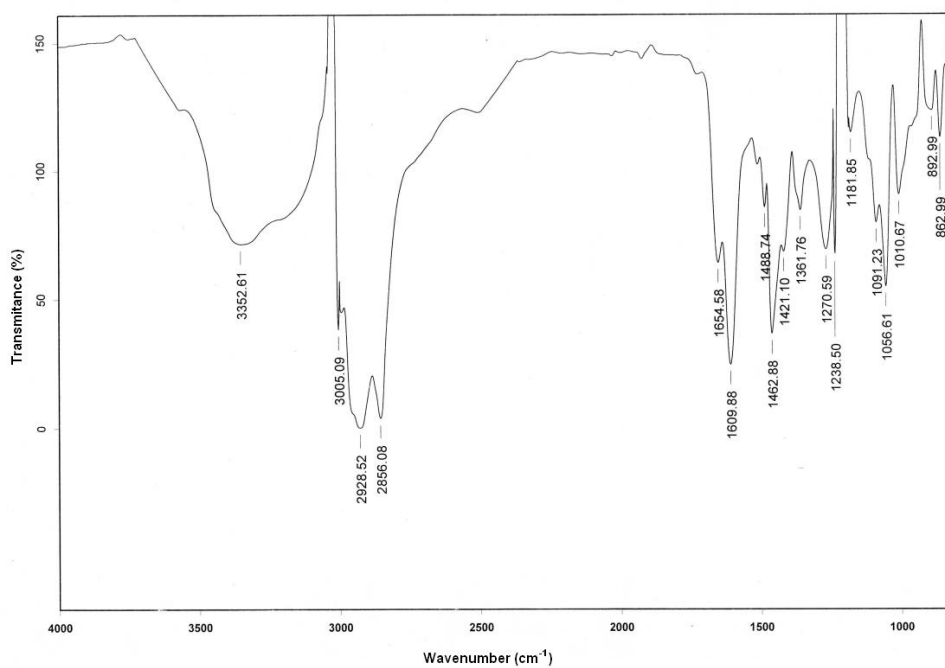


Figure 3. Infrared spectrum of coconut oil modified imidazoline (Inhibitor B).

Figs. 2-3 show the infra red spectra of both commercial and coconut oil-modified imidazoline respectively. It can be seen that the adsorption bands correspond to the same functional groups in both inhibitors and the chemical structure is virtually the same. Adsorption bands in the $3500\text{-}3100\text{ cm}^{-1}$, correspond to the $\nu_{\text{N-H}}$ peaks in tension for the primary and secondary amine/amide groups. The peaks which correspond to the $\nu_{\text{C-H}}$ groups in tension are $\nu(3009\text{ cm}^{-1})$, $\nu(2924\text{ cm}^{-1})$, $\nu(2854\text{ cm}^{-1})$ for both inhibitors. Peaks within the range $1650\text{-}1550\text{ cm}^{-1}$ correspond to the peaks $\nu_{\text{N-H}}$ in bending for the primary and secondary amine/amide groups. Peaks present at $\sim 1400\text{-}700\text{ cm}^{-1}$ correspond to the C-O-H and O-H groups. Finally, the adsorption peaks for C-H, ($3000\text{-}2850\text{ cm}^{-1}$ and $3100\text{-}3000\text{ cm}^{-1}$) correspond to the hydro carbonated chain present in each inhibitor.

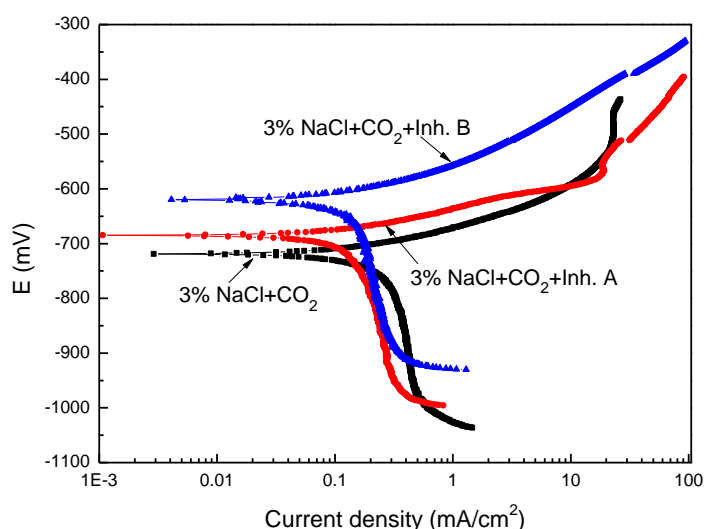


Figure 4. Effect of inhibitors A and B on the polarization curves in the CO_2 -containing 3% NaCl solution at 50°C .

Polarization curves for carbon steel in the different CO_2 -saturated 3% NaCl solutions are shown in Fig. 4, where it can be seen that the increase of polarization potential accelerates the dissolution of metal not only on the surface without adsorbed species but also the surface with adsorbed inhibitive species because the adsorbed species becomes unstable at a high polarization potential. The adsorbed inhibitor species will depart metal surface quickly due to the anodic dissolution of the metal. The E_{corr} value for the uninhibited solution was around -720 mV , but as soon as the inhibitors were added it became nobler, reaching values of -690 and -620 mV for inhibitor A and B respectively. The corrosion current density value was decreased when both inhibitors were added, decreasing the value from 0.31 mA/cm^2 down to 0.15 mA/cm^2 and 0.14 mA/cm^2 for both inhibitors. Inhibitor efficiency were very similar for both inhibitors, being slightly higher for commercial inhibitor than the coconut oil modified (table 1).

Table 1. Electrochemical parameters obtained from the polarization curves.

Solution	E_{corr} (mV _{SCE})	i_{corr} (mA/cm ²)	Inhibitor efficiency (%)
3% NaCl+ CO ₂	-720	0.31	-----
3% NaCl+ CO ₂ + inh. B	-690	0.15	51
3% NaCl+ CO ₂ + inh. A	-620	0.14	55

The change in the polarization resistance value with time, R_p , for the uninhibited and inhibited CO₂-saturated 3% NaCl solution is shown in Fig. 5.

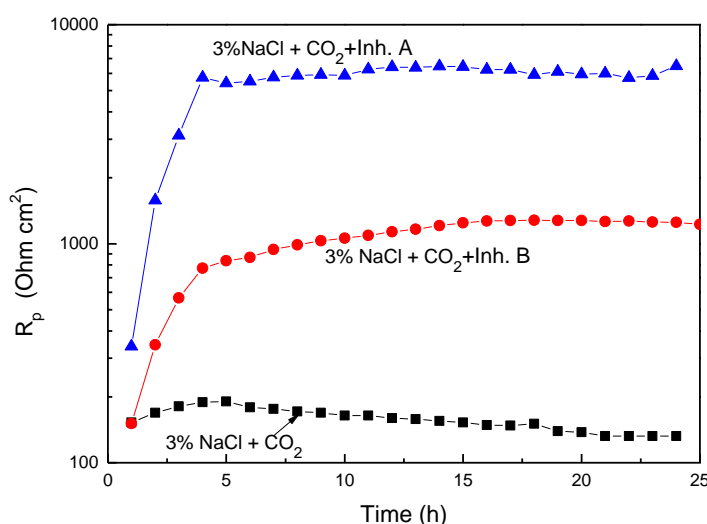


Figure 5. Effect of inhibitors A and B on the change of the R_p value with time in the CO₂-containing 3% NaCl solution at 50°C.

This figure shows that the lowest R_p value, and thus the highest corrosion rate, was shown by the uninhibited solution, and the highest R_p value, the lowest corrosion rate, was obtained with the commercial imidazoline, more than one order of magnitude. Coconut oil-modified imidazoline exhibited R_p values much higher than that for uninhibited solution, but lower than that obtained with the commercial inhibitor. The fact that the R_p values for both imidazolines increase at the beginning and after some time they reach a steady state value indicates the establishment of a protective stable film. The efficiency values calculated by using 2 is shown in Fig.6, indicating that the highest imidazoline exhibited efficiency values close to 500% whereas the coconut oil-modified imidazoline had efficiency values around 85%, which is an acceptable value.

This decrease in the corrosion rate in presence of CO₂ has been attributed to the formation of an iron carbonate, FeCO₃, film which is affected by iron and carbonate concentrations and temperature. All authors agree that by increasing the temperature would improve the protectiveness of the FeCO₃

scales as well as its adherence and hardness [30-33]. The lowest temperature necessary to obtain FeCO_3 films that would reduce the corrosion rate is 50°C .

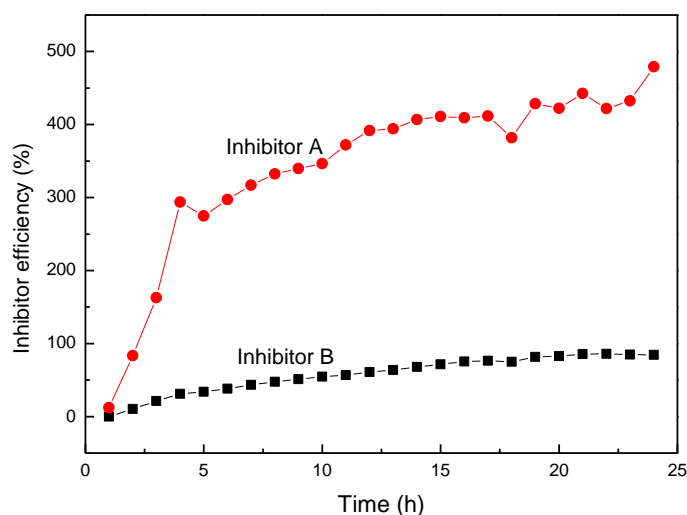


Figure 6. Change in the inhibitor efficiency with time for inhibitors A and B in a CO_2 -saturated 3% NaCl solution at 50°C .

On the cathodic branch, a cathodic limiting current can be seen, which is due to the hydration of CO_2 to give carbonic acid as follows [21]:



Since the solution is de-aerated, the dominant cathodic reactions are the reduction of H^+ ions, dissociation of carbonic acid [22-28]:



and water reduction:



The main anodic reaction, in absence of inhibitor, is iron dissolution according to:



though it may be through several steps. During this corrosion process, a corrosion scale of iron carbonate, FeCO_3 , would form on the surface of carbon steels according to [29]:

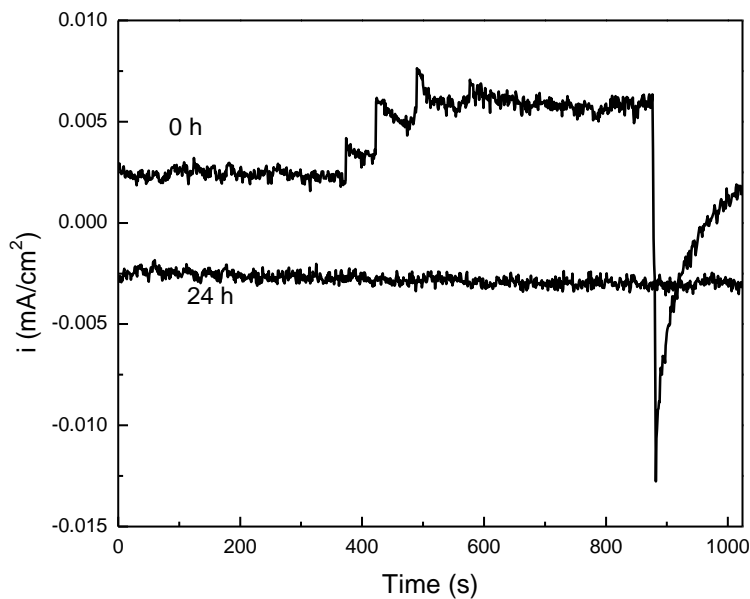


Figure 7. Noise in current for carbon steel exposed to the CO_2 -containing 3% NaCl solution at 50°C at different exposure times.

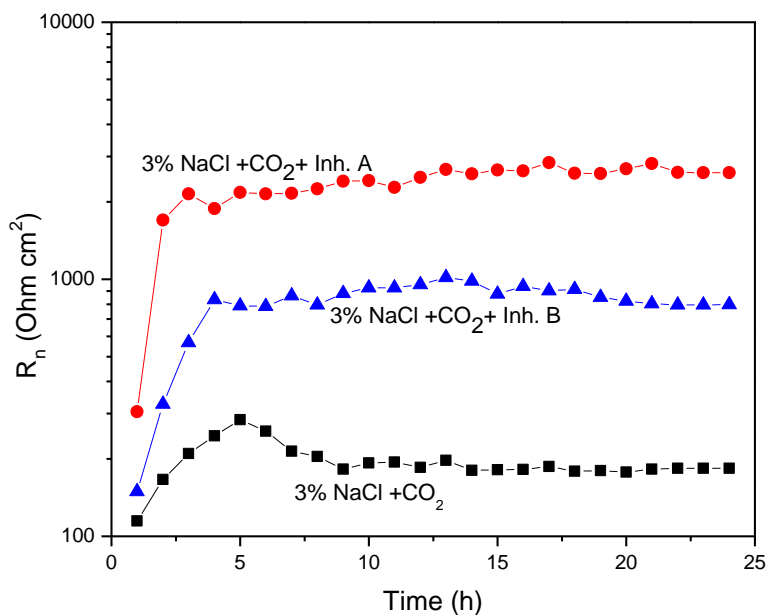


Figure 8. Effect of inhibitors A and B on the change of the R_n value with time in the CO_2 -containing 3% NaCl solution at 50°C .

As an example of the electrochemical noise readings, Fig. 7 shows the time series for the noise in current measurements in the 3% NaCl+CO₂ solution at the beginning of the experiment and after 24 hours of testing. Time series at the beginning of the experiment shows transients of low intensity and high frequency, typical of a material undergoing uniform type of corrosion, together with some transients with a sudden increase in intensity and a slow decay with low frequency are present, which are typical of a localized type of corrosion. According to [26], an increase in current is attributed either to film rupture or to pit nucleation, while the subsequent decrease in current is attributed to the recovery of a passive film without pit propagation and indicates a tendency towards localized corrosion. By using the ratio of the potential noise standard deviation, σ_v , over current noise standard deviation, σ_i , the noise resistance, R_n , was calculated and the results are shown in Fig. 8. This figure shows that the lowest R_n value corresponds to the pure 3% NaCl + H₂S solution with a value which remains constant throughout the experiment. When both inhibitors were added to the system, the R_n increased for more than one order of magnitude, reaching the highest value with the addition of inhibitor A. However, the R_n value for both inhibitors decreased rapidly reaching a steady state value around 5 hours or so. For inhibitor A the steady state R_n value was the highest, indicating the lowest corrosion rate. If we compare the behavior of R_n from Fig. 8 and that for R_p from Fig. 5 we can see that is very similar, which is very encouraging, since similar results are obtained by using different techniques. It is interesting to note that, both R_p and R_n values for the uninhibited solution increases during the first 5 hours or so, but after this time their value decreases as time elapses. The fact that both R_p and R_n values increase and after some time they decrease means that the iron carbonate film increases in thickness, reaches a maximum value and after that time it is detached from the steel surface.

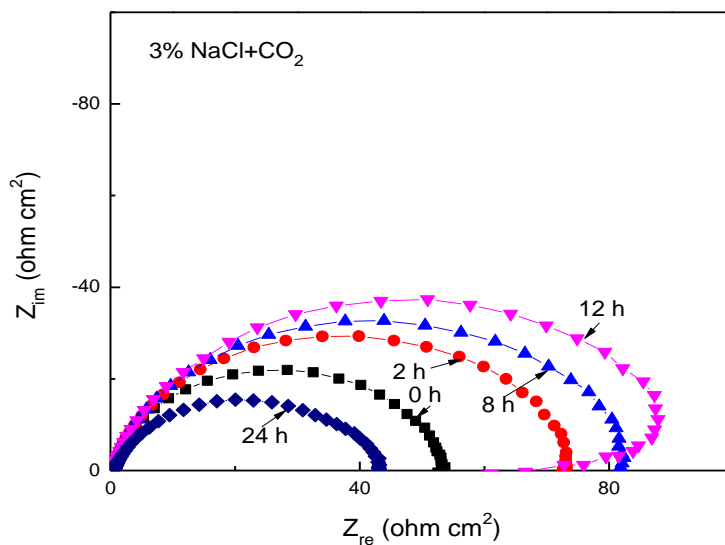


Figure 9. Nyquist diagrams for uninhibited CO₂-saturated 3% NaCl + CO₂ solution.

On the contrary, for the inhibited solutions, both R_p and R_n values increase continuously throughout the time, indicating a film formed by the inhibitor very stable. Thus, noise transients can

give us information not only about the type of corrosion that is taken place on a metal surface but also about the film formation process and its evolution with time.

Nyquist diagram for carbon steel exposed to a CO₂-saturated 3% NaCl solution at 50 °C is shown on Fig. 9, where it can be seen that the data describe a depressed, capacitive-like semicircle, with its centre at the real axis, indicating that the corrosion process is under charge transfer control from the metal surface to the environment through the double electrochemical layer. The high frequency semicircle diameter corresponds to the charge transfer resistance, R_{ct} , equivalent to the polarization resistance, R_p , thus inversely proportional to the corrosion current density, i_{corr} . As time elapses, the semicircle diameter increases but after 12 hours it decreases, increasing, thus, the corrosion rate, showing the non-protective nature of the corrosion products. CO₂ corrosion of carbon and low alloy steels is strongly dependent on the surface formed films during the corrosion processes. The protectiveness, rate of formation/precipitation, and the stability of the film controls the corrosion rate and its nature. The main formed film during CO₂ corrosion of iron and low alloy steels is iron carbonate, FeCO₃, which is affected by iron and carbonate concentrations and temperature. Thus, it seems that FeCO₃ film remains on the steel surface a short time period, and after this time, the corrosion rate increases.

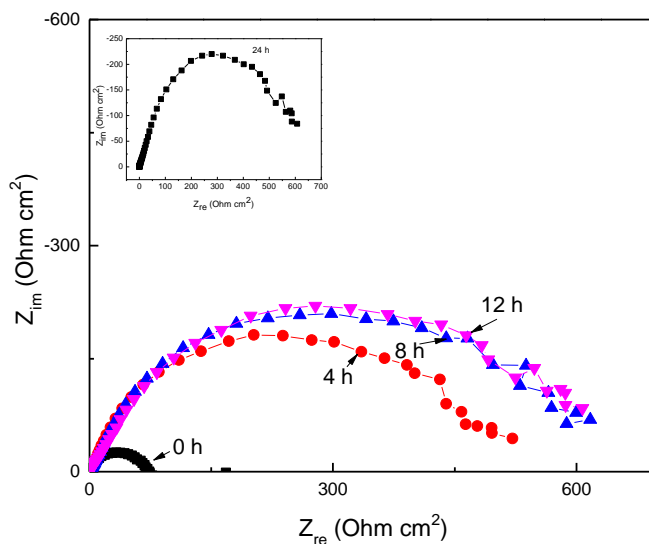


Figure 10. Nyquist diagrams for CO₂-saturated 3% NaCl + CO₂ solution, containing inhibitor A.

When both inhibitors are added to the CO₂-saturated 3% NaCl solution, data describe a single capacitive-like depressed semicircle with its center at the real axis, indicating that the corrosion process is under charge transfer control from the steel to the electrolyte through the double electrochemical layer, Figs. 10-11. However, the semicircle diameter is almost ten times of magnitude higher than that for uninhibited solution by adding commercial imidazoline (inhibitor A), Fig. 10, and almost four times higher by adding the coconut oil-modified imidazoline (inhibitor B), Fig. 11.

However, unlike the uninhibited solution, the semicircle diameter obtained with both inhibitors reach a final steady value, indicating the protective nature of the film formed by adding both inhibitors.

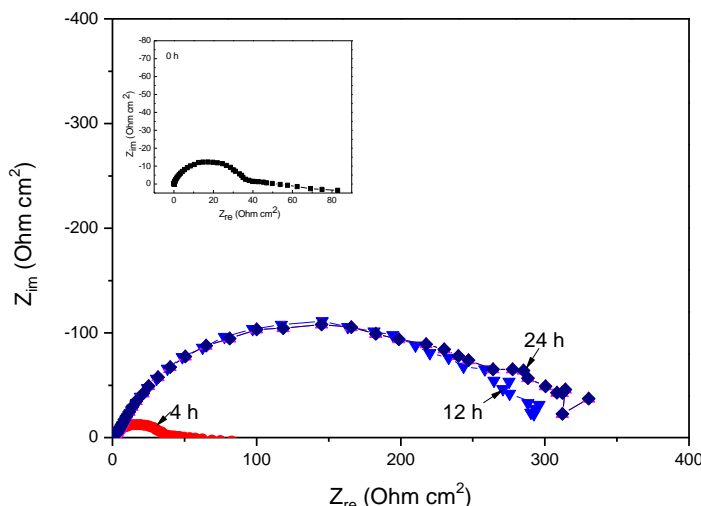


Figure 11. Nyquist diagrams for CO_2 -saturated 3% NaCl + CO_2 solution containing inhibitor B.

The fact that the semicircle diameter was bigger for commercial inhibitor than that for the coconut oil-modified one shows that the corrosion rate is lower with the former than the later, as shown by the R_p and R_n values, Figs. 5 and 8, however, the decreases in the corrosion rate obtained with the modified inhibitor is quite acceptable, which is very encouraging because provides very promising results in the preparation of green corrosion inhibitors.

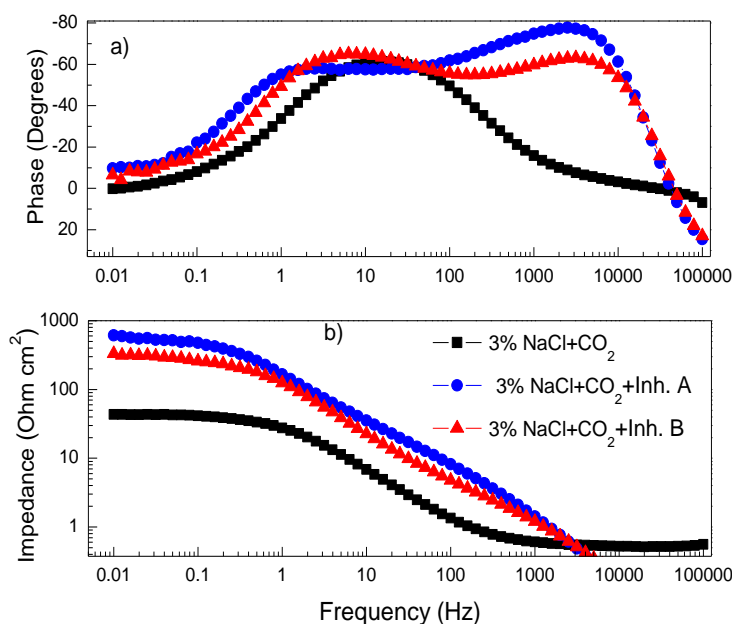


Figure 12. Bode plots in the a) phase and b) impedance format for carbon steel in the CO_2 -saturated solution with and without inhibitors A and B.

Fig. 12 shows Bode diagrams in both impedance and phase angle formats for all the tested solutions at the beginning of the experiment. Bode diagrams in the phase angle format, Fig. 12 a, shows the presence of only one peak for the uninhibited CO_2 -saturated 3% NaCl solution, but either with the addition of inhibitors A or B there are two well defined peaks at 10 and 1000 Hz. The presence of two peaks indicates the formation of a protective corrosion products layer. Impedance plots, Fig. 12 b, show that the lowest impedance or modulus corresponds to the uninhibited CO_2 -saturated 3% NaCl solution, whereas the highest value, more than one order of magnitude, was obtained with the addition of inhibitor A.

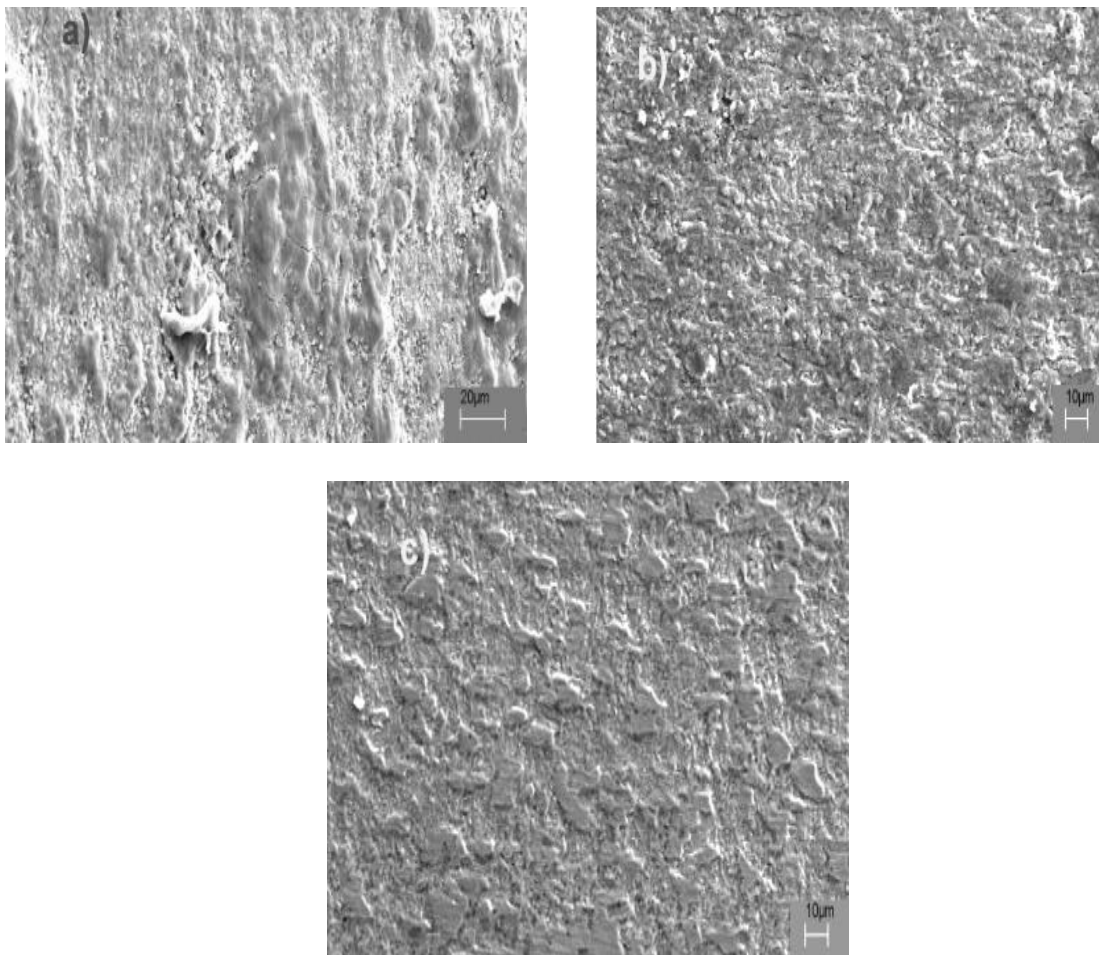


Figure 13. Micrograph of corroded surface of carbon steel exposed to a) 3% NaCl+ CO_2 b) 3% NaCl+ CO_2 + Inh. A and c) 3% NaCl+ CO_2 + Inh. B.

Some micrographs of corroded specimens in the uninhibited and inhibited CO_2 -saturated 3% NaCl solutions are shown in Fig. 13. The steel corroded in the uninhibited solution shows porous corrosion products, maybe iron carbonate, FeCO_3 , film, with some cracks, where the electrolyte can penetrate and corrode the steel surface. On the other hand, the film found on the steel surface of the steel exposed solutions showed a more compact nature, forming an effective barrier against the ingress of the aggressive environment. The molecular structure of imidazoline, Fig. 1, is composed of a five member ring containing nitrogen elements, a C-14 saturated hydrophobic head group and a pendant,

hydrophilic carboxyamido group attached to one of the nitrogen atoms. The compound can be adsorbed on the metal surface by the formation of an iron-nitrogen co-ordination bond and by a pi-electron interaction between the pi-electron in the head group and iron [11-14]. Though not a primary contribution to the adsorption strength of the compound on the surface of the metal, coulombic attraction between the negative charge, i.e. electrons, on the metal surface (as a result of the specific adsorption of chloride ions) and the imidazoline derivative may also contribute to the inhibition ability of the compound. When the adsorbed inhibitor molecules exceed certain number of atoms on the surface and these molecules are close enough, electrostatic repulsion between the negative charge of the pendant group, leads to a desorption of the inhibitor molecules, leading to unprotected sites on the metal and an increase on the corrosion rate.

4. CONCLUSIONS

A commercial imidazoline-base corrosion inhibitor has been modified with coconut oil and its corrosion inhibition performance for carbon steel in a CO₂-saturated 3% NaCl solution at 50°C. It was found with different techniques that even with small concentrations such as 20 ppm the corrosion inhibition of the commercial imidazoline-based inhibitor are not reached by the modification with vegetable oil, since the efficiency of the coconut oil-modified imidazoline was around 85% whereas that for commercial one was higher than 400%. However, these results are very encouraging since they indicate that small doses of coconut-modified imidazoline could be used as a corrosion inhibitor.

ACKNOWLEDGEMENTS

The authors acknowledge D. Cuervo and DGAPA-UNAM for Ignacio Regla sabbatical fellowship at ICF-UNAM.

References

1. A. Ikeda, S. Mukai, M. Ueda, NACE Corrosion/84, Houston, Texas (1984) Paper No. 289.
2. X. Jiang, Y. G. Zheng, D. R. Qu, W. Ke, Corr. Sci. 48 (2006) 3091. S. Arzola, J. Genesca, J. Solid State Electrochem., 8 (2005), pp. 197–200
3. M. B. Kermani, A. Morshed. *Corrosion* 59 (2003) 659.
4. K. Videm, J. Kvarekval. *Corrosion* 51(1995) 260.
5. D. A. Lopez, W. H. Schreiner, S. R. de Sanchez, S. N. Simison. *Appl. Surf. Sci.* 207 (2003) 69.
6. S. L. Wu, A. D. Cui. F. He, Z. Q. Bai, S. L. Zhu, X. J. Yang. *Materials Letters*, 58(2004)1076
7. T. Hong, Y. H. Sun, W. P. Jepson. *Corros. Sci.* 44 (2002) 101.V.
8. J. B. Li, X. Hou, M.S Zheng, J. W. Zhu, *Int. J. Electrochem. Sci.*, 2 (2007) 607.
9. Ramachandran S and Jovancicevic V., *Corrosion* 55 (3) (1999) 259
10. Z. Xueyuan, *Corrosion Science* 43 (2001) 1417
11. F. Bentiss, M. Lagrenee, M. Traisnel, J.C. Hornez, *Corros. Sci.* 41, (1999) 789.
12. S. Ramachandran, M. Tsai, M. Blanco, H. Chen, W. A. Tang, Godard III *Langmuir* 12 (1996) 6419.
13. D. Wang, S. Li, M. Ying, M. Wang, Z. Xiao, Z. Chen, *Corros. Sci.*, 41 (1999) ; 1911.

14. F. Farelas, A. Ramirez, *Int. J. Electrochem. Sci.*, 5 (2010) 797.
15. Lijuan Feng, Huaiyu Yang, Fuhui Wang, *Int. J. Electrochem. Sci.*, 7 (2012) 4064.
16. Shuangkou Chen, Steve Scheiner, Tapas Kar, Upendra Adhikari, *Int. J. Electrochem. Sci.*, 7 (2012) 7128.
17. Luz Maria Rodriguez-Valdez, Alberto Martinez-Villafañe, Daniel Goltzman-Mitnik, *Theochem* 713 (2005) 65.
18. K. Bilkova, N. Hackerman, M. Bartos, Proceedings of NACE Corrosion/2002, NACE 2002, Denver, CO, paper No. 2284.
19. E. Sosa, R. Cabrera-Sierra, E. Marina, M.E. Rincon, M.T. Oropeza, I. Gonzalez, *Electrochimica Acta* 47 (2002) 1197.
20. H. Ashassi-Sorkhabi, S.A. Nobavi-Amri, *Electrochimica Acta* 47 (2002) 2239.
21. K.G. Gonroy, C.B. Breslin, *Electrochimica Acta* 48 (2003) 721.
22. S. Arzola, J. Mendoza-Florez, R. Duran-Romero, J. Genesca, *Corrosion*, 62 (2006) 433.
23. P.H. Tewart, A.B. Campbell, *Can. J. Chem.*, 57 (1979) 188.
24. F.H. Meyer, O.L. Riggs, R.L. McGlasson, J.D. Sudbury, *Corrosion*, 14 (1958) 69.
25. G.W. Walter, *Corros. Sci.*, 26 (1989) 681
26. S.H. Yoo, Y. W. Kim, K. W. Chung, S. Y. Baik, J. S. Kim, *Corros. Sci.*, 59 (2012) 42.
27. K. Hladky, J.L. Dawson, *Corros. Sci.* 22 (1982) 231.
28. H. Ma, X. Chang, G. Li, S. Chen, Z. Quian, S. Zhao, L. Niu, *Corros. Sci.* 42 (2000) 1669.
29. A J Szyprowski, *Corrosion* 59 (2003) 68.
30. S. Nesic, J. Postlethwaite, S. Olsen, *Corrosion* 52 (1996) 280.
31. C. de Waard, D.E. Milliams, *Corrosion* 31 (1975) 131-140.
32. G. Schmitt, B. Rothman, *Werkstoffe und Korrosion* 28 (1977) 816-825.
33. T. Hurlen, S. Gunvaldsen, R. Tunold, F. Blaker, P.G. Lunde, *J. Electroanal. Chem.* 180 (1984) 511-518.